

Research Article

Experimental Analysis and Discussion on the Damage Variable of Frozen Loess

Cong Cai,^{1,2} Wei Ma,¹ Shuping Zhao,³ and Yanhu Mu¹

¹State Key Laboratory of Frozen Soil Engineering, Cold and Arid Regions Environmental and Engineering Research Institute, Chinese Academy of Sciences, Lanzhou 730000, China

²University of Chinese Academy of Sciences, Beijing 100049, China

³Key Lab of Visual Geographic Environment, Ministry of Education, Nanjing Normal University, Nanjing 210023, China

Correspondence should be addressed to Wei Ma; cc20109163@163.com

Received 25 October 2016; Revised 2 January 2017; Accepted 8 February 2017; Published 13 March 2017

Academic Editor: Paulo M. S. T. De Castro

Copyright © 2017 Cong Cai et al. This is an open access article distributed under the Creative Commons Attribution License, which permits unrestricted use, distribution, and reproduction in any medium, provided the original work is properly cited.

The damage variable is very important to study damage evolution of material. Taking frozen loess as an example, a series of triaxial compression and triaxial loading-unloading tests are performed under five strain rates of 5.0×10^{-6} – 1.3×10^{-2} /s at a temperature of -6°C . A damage criterion of frozen loess is defined and a damage factor D_c is introduced to satisfy the requirements of the engineering application. The damage variable of frozen loess is investigated using the following four methods: the stiffness degradation method, the deformation increase method, the dissipated energy increase method, and the constitutive model deducing method during deformation process. In addition, the advantages and disadvantages of the four methods are discussed when they are used for frozen loess material. According to the discussion, the plastic strain may be the most appropriate variable to characterize the damage evolution of frozen loess during the deformation process based on the material properties and the nature of the material service.

1. Introduction

There are many defects in a material, such as voids and cracks, which may constantly grow and accumulate under external loads. These inner defects and their change processes under external loads are defined as the damage and the damage evolution of material [1]. The damage evolution can also be considered the degradation of material properties. Xu introduced a continuous variable and an evaluation law to describe the rupture process of metal materials under the creep process [1]. Since then, many achievements in the damage evaluation of materials were obtained [2–6], and a new discipline in solid mechanics has been developed, which is named continuum damage mechanics (CDM).

In general, the main methods of characterizing the damage and damage evolution of a material are the mesomethod based on material science (metal physics), the macromethod based on phenomenology, and the micromethod based on statistics. The study covers the following three major components: selection of the damage variable, definition of the

damage threshold value, and establishment of the damage evolution law. However, because of the randomness of the defects, it is too difficult to consider the effects of all defects on the degradation of material properties under external loads. Therefore, the most common investigation method of damage mechanics is to introduce a continuous variable, which can describe the changing process of microstructure defects during deformation process. Then, the changes in effective loading area or macromechanical properties of the material under loads are characterized; thus, this continuous variable is also called the damage factor [7]. The damage variable is introduced to describe the change of the damage factor. An appropriate damage variable should include three features. First, it must have a direct response to the mesoscopic changes of the material. Second, the damage variable of different materials should select this physical index, which can directly or indirectly characterize the main property of the material. Third, the selected variable better can be directly obtained from the experiment. Before selecting the damage

TABLE I: Grain size distribution and physical properties of frozen loess.

Grain size distribution of loess in Lanzhou/%			Initial moisture	Liquid limit	Plastic limit
0.05–0.075 mm	0.005–0.05 mm	<0.005 mm	/%	/%	/%
23.88	66.57	9.55	6.40	15.70	24.30

variable and establishing the damage evolution law, the initial criterion of damage (entering the damage status) and failure criterion of damage (damage thresholds of material) should be defined. The theory was first introduced to study the material uniaxial tension: $D = 0$, undamaged state; $D = 1$, failure state; and $0 < D < 1$, damaged intermediate state [8]. Voyiadjis also raised a key issue concerning damage of different materials: “What is failure?” [9]. According to Voyiadjis, the failure criteria of different materials ($D = 1$) should be clearly defined by considering the material properties and purposes of engineering applications; otherwise, the definition of the damage variable will lose its meaning. According to the ideal condition, the failure criterion of material is that the effective stress of the material reaches the residual strength value. However, for engineering applications, considering the unpredictable loads and structural instability, the situation that cannot satisfy safety requirements will appear even if the stress conditions do not reach failure conditions (the residual strength) [1]. For engineering requirements, CDM often provides a critical damage D_c to represent failure conditions. Based on the abovementioned developments, researchers have proposed many different methods, such as the stiffness degradation [10], dissipated energy increase [11], and development of plastic strain [12]. Lapovok [12] and Shi et al. [13] studied the damage evolution of metal by deformation and density variation. Cao et al. studied the damage evolution of rock using the digital speckle correlation method (DSCM) and compared with the results from computed tomography (CT) [14]. Swoboda and Yang considered that the dissipated energy could be turned as the driving force of crack growth based on the view of Griffith crack in fracture mechanics under the isothermal and insulate condition [11]. In addition, the constitutive model of some materials has been obtained, but it cannot clearly observe the damage evolution law. Then, the law can be derived by the theory of effective stress [7, 15].

However, few studies compared the advantages and disadvantages among different damage variables or discussed the selection criteria of the damage variable to the same material. In this paper, the frozen loess is a typical complex material with a four-phase medium [16], which is notably sensitive to environmental conditions. In addition, the microdefects are difficult to describe because of the complexity of the material structure. Thus, many microtest methods, including CT and scanning electron microscope (SEM), cannot be used for their damage testing [5]. At present, the common method of damage research of frozen loess depends on the macroexperimental results. This paper studies the damage evolution of frozen loess under external loads based on a series of triaxial test results on frozen loess; the evolution characteristics of different damage variables during deformation are investigated and compared.

The comparison analysis is also conducted by using different damage factors to evaluate the mechanical properties of frozen loess based on experimental results and previous studies.

2. Specimen Preparation and Test Conditions

Loess soils from Jiuzhoutai town (a seasonal frozen region) of Lanzhou City, northwest China, are used in this study. The particle size distribution and associated physical parameters of the soils are shown in Table I. To ensure the uniformity, the soil specimens are prepared according to the following steps: air drying of the undisturbed soils, crushing and 2 mm screening, measuring the initial moisture content, mixing to obtain a 16.5% moisture content, and maintaining that content for 6 h without evaporation. The specimens are compacted using variable loading rates in a cylinder. The dimensions of the specimens are 61.8 mm in diameter and 125.0 mm in height. After the compaction, the specimens are completely saturated using distilled water in vacuum conditions for 10 h. Then, they are put into rigid molds and quickly frozen at a low temperature of -25°C for over 48 h to limit water loss and migration. After the freezing, the specimens are taken from the molds and mounted with epoxy resin platens on both ends and covered with rubber sleeves. Finally, the specimens are kept in an incubator for over 12 h until the specimens reached the target testing temperature of -6°C [17].

Two types of mechanical tests are conducted using a material testing machine (MTS-810): constant strain rate triaxial compression (C) and loading-unloading compression (L-U-C). All tests are performed at a constant confining pressure ($\sigma_3 = 0.1 \text{ MPa}$) and a constant temperature ($T = -6^{\circ}\text{C}$). The strain rates of the tests are $1.3 \times 10^{-2}/\text{s}$, $5.0 \times 10^{-3}/\text{s}$, $5.0 \times 10^{-4}/\text{s}$, $5.0 \times 10^{-5}/\text{s}$, and $5.0 \times 10^{-6}/\text{s}$. The loading and unloading tests are performed at the identical strain rate to avoid the effect of the strain rate on the same trial.

3. Results and Analysis

The C test results under five different strain rates are shown in Figure 1. The deviator stress ($\sigma_1 - \sigma_3$) and axial strain (ϵ_1) relation of frozen loess strongly depends on the strain rate. At small strain, the stress-strain behavior performs as hardening. With the continuous loading, the specimen damage gradually develops and the stress-strain behavior performs as strain softening. With the increase in strain rate, the peak axial strain ϵ_1^u sharply increases and approaches the maximum at a strain rate of $5.0 \times 10^{-3}/\text{s}$. Then, the peak axial strain decreases with the strain rate increase, as shown in Figure 2. This result suggests that the damage of frozen loess is strain-dependent and strongly rate-dependent. Variations

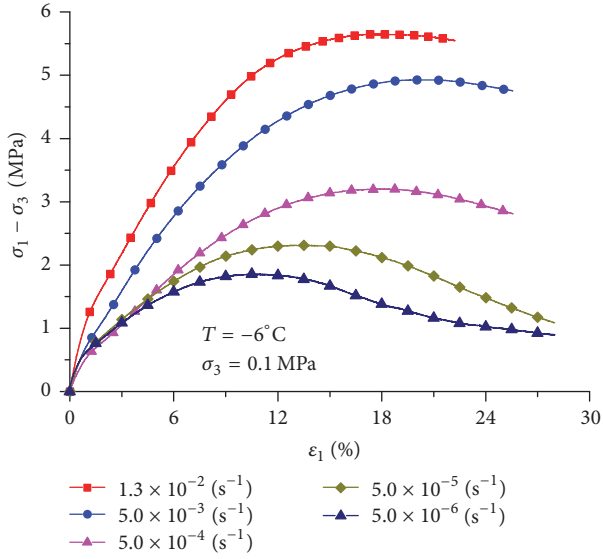


FIGURE 1: Deviator stress-axial strain curves for frozen loess under C tests.

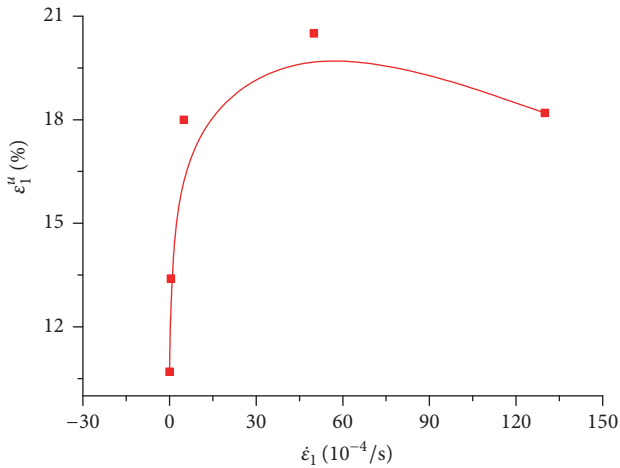


FIGURE 2: Peak strain for frozen loess under C tests.

of the stress-strain relations and the peak axial strains with the strain rates are related to the rheological characteristics of frozen loess.

The *L-U-C* test results under the five different strain rates are shown in Figure 3, and the comparison of *C* and *L-U-C* test results is shown in Figure 4. It can be seen that the loading and unloading cycles test do not affect the deformation behavior of frozen loess. To verify the accuracy of the test data, some repeated tests are carried out, as shown in Figure 5.

4. Damage Features of Frozen Loess

In this paper, the following studies are conducted on the premise of the phenomenism and isotropic continuum medium. The changes of the mesofabric are characterized by

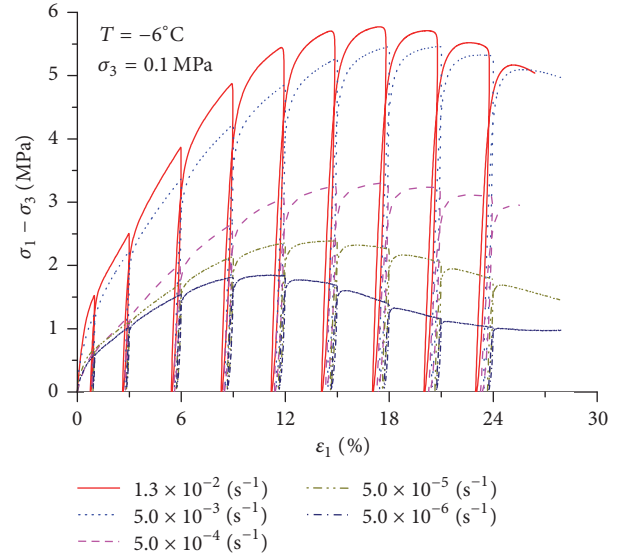


FIGURE 3: Deviator stress-axial strain curves for frozen loess under *L-U-C* tests.

introducing a continuous variable. Then, the macro description of damage accumulation can be expressed by a scalar equation as follows [12, 18]:

$$D = D(\sigma_{ij}, \epsilon_{ij}, \dot{\epsilon}_{ij}). \quad (1)$$

There were different damage variables with different damage evolution laws even when the identical physical process is described. The concept of damage variable was first introduced from the concept of effective stress, which was proposed by Kachanov [19].

$$\sigma_{\text{eff}} = \frac{\sigma_0}{1-D}. \quad (2)$$

Then, the damage evolution law can be written as

$$\frac{dD}{dt} = f(D, \sigma_{ij}), \quad (3)$$

where D is the damage variable; σ_{eff} is the effective stress; and σ_0 is the nominal stress. If a reasonable damage evolution law can be established, then the damage state, residual strength, and longevity of material can be easily and accurately predicted.

4.1. Damage Criterion of Frozen Loess. According to the studies of Zhao et al. [5], Xu et al. [6], and Huang and Li [20] and the test results of this study, the material is softening when the deformation reaches a certain level. Then, the cracks in the material expand rapidly, the strength decreases rapidly, and the structure becomes unstable. Therefore, some researchers proposed that the failure condition of material could be defined as the status that the stress reaches the extreme value point [1]. The status can be expressed as follows:

$$\left. \frac{d\sigma}{d\epsilon} \right|_{D_c} = 0. \quad (4)$$

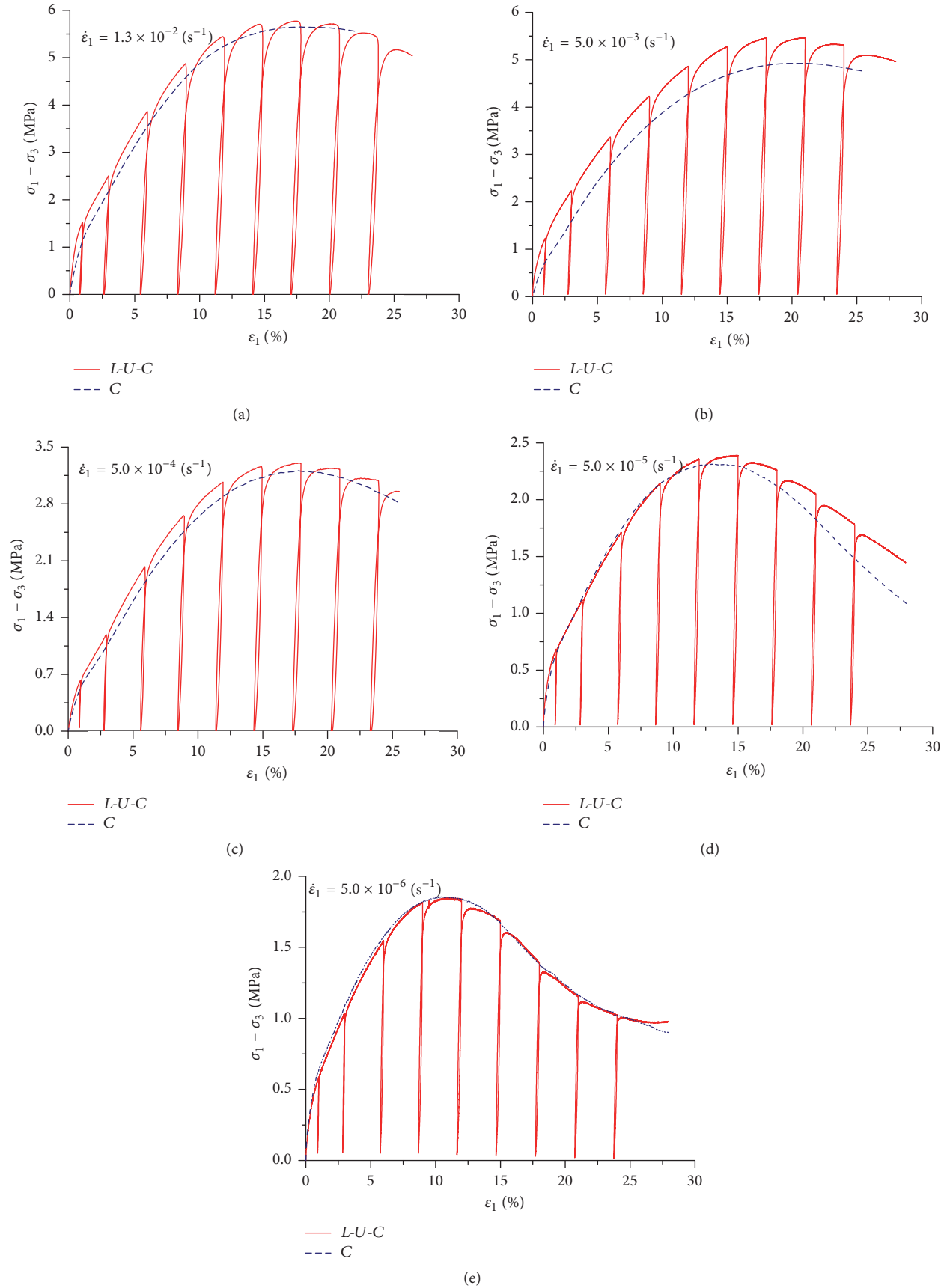


FIGURE 4: The comparison of *C* and *L-U-C* tests under different strain rates.

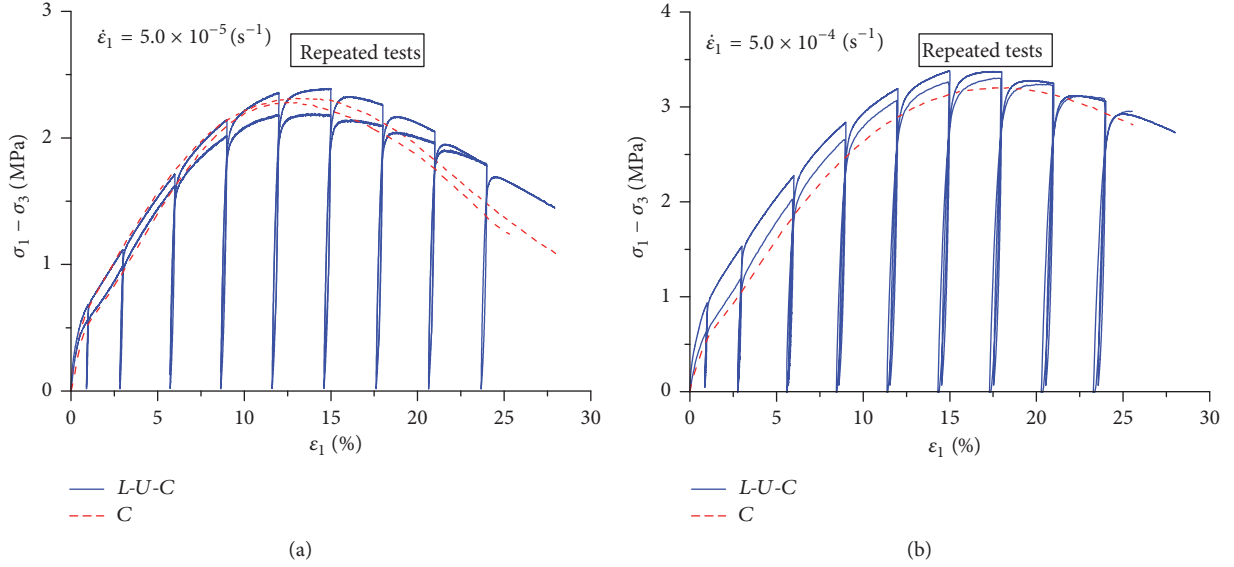


FIGURE 5: The accuracy of the test data.

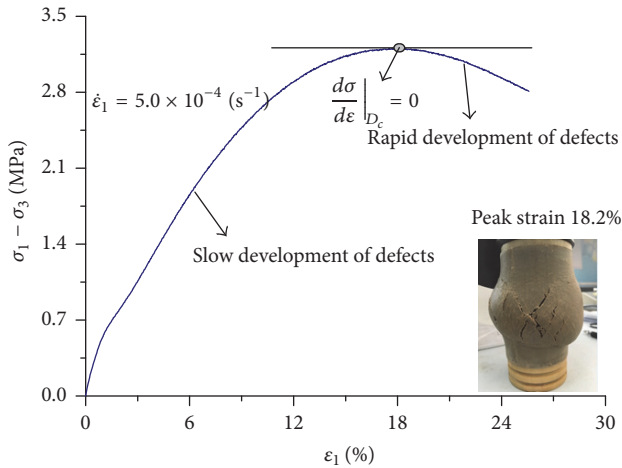


FIGURE 6: The selected criterion of critical damage for frozen loess.

Based on a series of repeated tests, the peak strain of frozen loess is obtained under different strain rates according to the statistics principle. The new test is accomplished when the strain reaches the peak strain. The typical physical status of frozen loess around the peak strain is shown in Figure 6. The cracks on the frozen loess surface are large and rapidly develop after the peak strain. Thus, this status is unsuited for continuous loading and can be referred to as the critical damage status of frozen loess material.

In addition, the selection of the damage factor and quantitative relationship between the damage factor and the damage variable should be considered. Based on previous studies and the test results of this study, this paper discusses four common damage factors and damage variables.

4.2. Damage Variables of Frozen Loess

4.2.1. Stiffness Degradation Method. The stiffness of the material continuously degenerates with the increase of deformation. The degradation of mechanical properties of the material is due to the nucleation and development of the material damage at the microscale level, such as voids and cracks. According to the above discussions and previous studies [8, 10, 21], the unloading modulus is selected to characterize the stiffness of the material under different damage states. Then, the damage variable can be written as follows:

$$D = 1 - \frac{\tilde{E}}{E_0}, \quad (5)$$

where E_0 is the initial elastic modulus of the material, which is also known as the undamaged modulus. \tilde{E} is the elastic modulus under different damage state.

To obtain the component of the elastic strain ϵ_1^e , plastic strain ϵ_1^p , and the change law of unloading modulus during the deformation, the hysteretic loop is addressed using the approximation-linearized method [22], as shown in Figure 7.

There are two selections for the unloading modulus: modulus of hysteretic loop E_h and the secant modulus E_s . The variations of E_h and E_s with the axial strain are shown in Figures 8(a) and 8(b), respectively.

In Figure 8, the unloading modulus of frozen loess decreases with the increase in axial strain when the strain rate is below $5.0 \times 10^{-4}/s$, but the change trend is not obvious when the strain rate is above $5.0 \times 10^{-4}/s$. The phenomenon is verified by repeated tests. According to Xie [23] and Yu [24], the unloading modulus was selected as a damage factor based on the equivalence hypothesis of strain and the method of elastic modulus. However, this hypothesis can only be

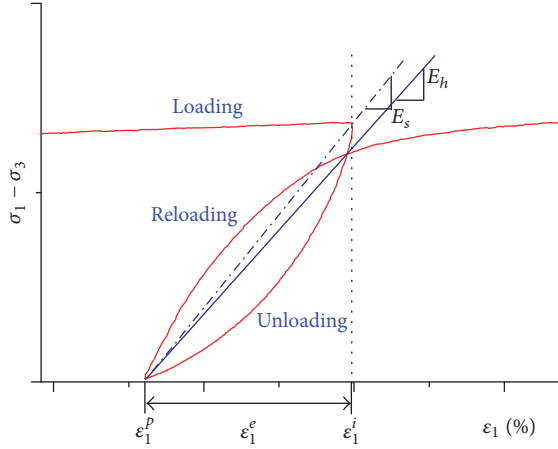


FIGURE 7: The decoupling principle on the hysteretic loop.

applied for elastic damage. The frozen loess is an elastic-plastic coupling material, which can be verified from the L - U - C tests that the plastic deformation is dominant even if the axial strain is 1%. Thus, the actual damage feature of frozen loess is significantly simplified or hidden when the unloading modulus is selected as the damage factor.

Many experimental results show that the unloading modulus can only decrease when the deformation reaches a certain status [23]. This phenomenon suggests that there is a damage threshold value for elastic-plastic materials, which is consistent with the law that the granular material is first compacted, and subsequently shear failure under external loads. The unloading modulus may be greater than or equal to the initial elastic modulus of the material before this certain status. Then, using the unloading modulus (E_h or E_s) to calculate the material damage will lead to a wrong conclusion; for example, no damage or even negative damage occurs. However, for the unloading modulus, E_s may be better than E_h because E_s is only a part of the unloading curve.

To study the stiffness degradation of the material during the deformation, some researchers proposed that the deformation modulus should be adopted, which is defined as the slope of the secant line of the stress-strain curve from the loading point to the instantaneous damage point (see Figure 9) [24–26]. The deformation modulus E_d is used to describe the damage evolution of the material.

The evolution law of E_d with axial strain under different strain rates is shown in Figure 10. The damage variable is expressed as follows:

$$D = 1 - \frac{E_d}{E_0}. \quad (6)$$

In addition, there is a quantitative relationship between the unloading modulus E_s and the deformation modulus E_d under the same strain and stress [23]:

$$E_d = \frac{\varepsilon_1 - \varepsilon_1^p}{\varepsilon_1} E_s, \quad (7)$$

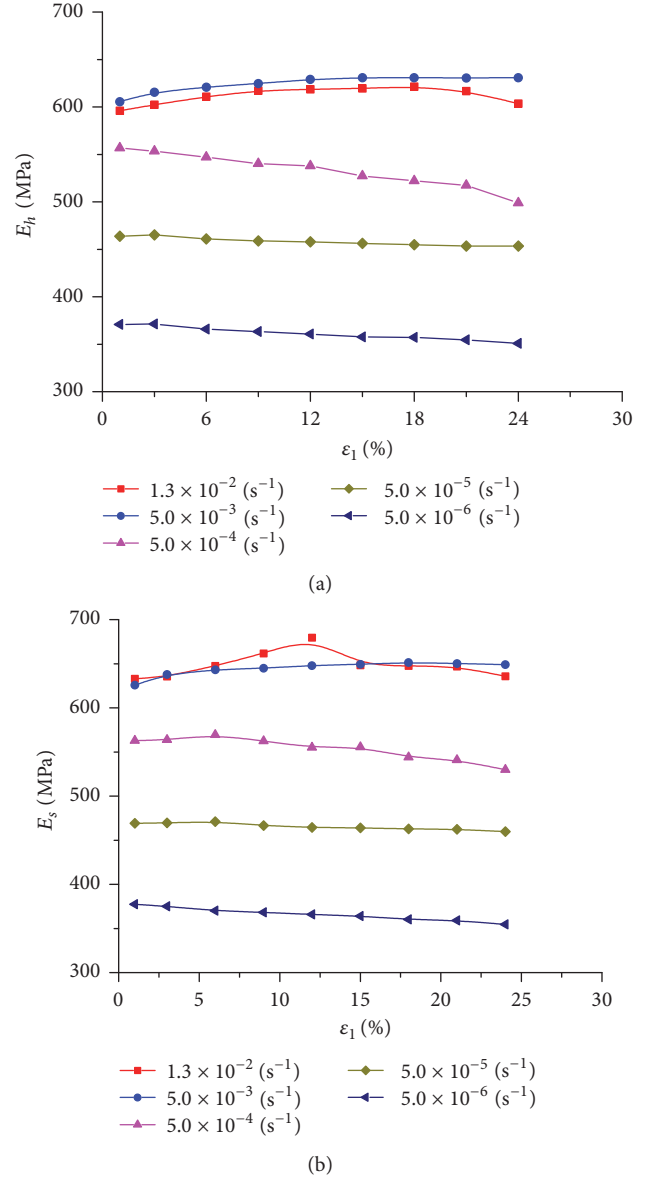


FIGURE 8: Variation of E_h and E_s with axial strain under different strain rates.

where ε_1^p is the axial plastic strain. Then, the damage variable can be described with the unloading modulus (E_s).

$$D = 1 - \frac{\varepsilon_1 - \varepsilon_1^p}{\varepsilon_1} \left(\frac{E_s}{E_0} \right). \quad (8)$$

Then, the unloading modulus (E_s) can describe the increase in damage and the stiffness degradation of material like the deformation modulus (E_d). Based on the test results of this study, the relationship between axial strain and damage variable is established as follows:

$$D = \frac{\varepsilon_1}{a\varepsilon_1^2 + b\varepsilon_1 + c}, \quad (9)$$

where a , b , and c are material parameters corresponding to the strain rate. The test results and fitting curves are shown in

TABLE 2: Material parameters a , b , and c under different strain rates (stiffness).

$\dot{\varepsilon}_1$	$1.3 \times 10^{-2}/s$	$5.0 \times 10^{-3}/s$	$5.0 \times 10^{-4}/s$	$5.0 \times 10^{-5}/s$	$5.0 \times 10^{-6}/s$
a	-0.381	-0.377	-0.544	-0.463	-0.532
b	1.142	1.150	1.189	1.134	1.127
c	0.014	0.009	0.003	0.005	0.004

TABLE 3: Material parameter θ under different strain rates (plastic strain).

$\dot{\varepsilon}_1$	$1.3 \times 10^{-2}/s$	$5.0 \times 10^{-3}/s$	$5.0 \times 10^{-4}/s$	$5.0 \times 10^{-5}/s$	$5.0 \times 10^{-6}/s$
θ	5.520	4.710	5.448	7.241	9.075

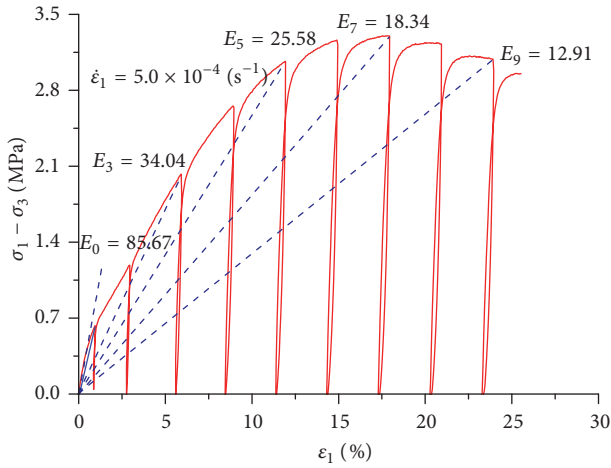
FIGURE 9: The definition of deformation modulus E_d .

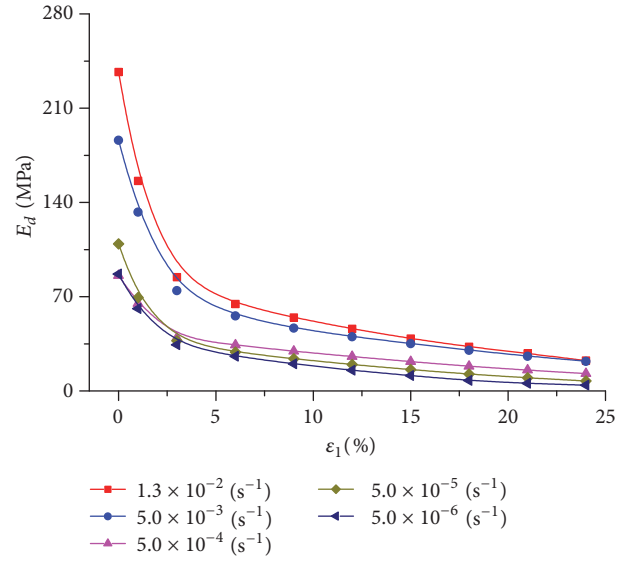
Figure 11, and the parameters a , b , and c under different strain rates are listed in Table 2.

4.2.2. Plastic Strain Method. Considering the process of fatigue damage, Lemaitre [27] and Lapovok [12] proposed that plastic strain or permanent strain was an irreversibility macroscopic behavior as a result of microcrack growth and development (damage-fatigue equivalent analogy method). Therefore, the plastic deformation can be selected as the damage factor according to the ability of the material to resist permanent deformation. Then, according to Liao et al. [28], the damage variable can be written as follows:

$$D = 1 - \exp\left(-\frac{\varepsilon_1^p}{\varepsilon_1^u}\right), \quad (10)$$

where ε_1^u is the peak strain (see Figure 2) and ε_1^p is plastic strain under different deformation statuses.

The variation of ε_1^p with axial strain under different strain rates is shown in Figure 12. Within the total deformation, the plastic strain is dominant, and the elastic deformation contributes very little. In addition, the development of plastic strain is almost independent of the strain rate. Based on the test results of this study, the relationship between the damage variable and the axial strain is shown in Figure 13.

FIGURE 10: Variation of E_d with axial strain under different strain rates.

Liao et al. introduced the following negative exponential function in order to establish the relationship of the damage variable and the axial strain [28]:

$$D = 1 - \exp(-\theta\varepsilon_1), \quad (11)$$

where θ is a material parameter corresponding to time, which controls the damage degree and degradation of material properties. Parameter θ under different strain rates is listed in Table 3 according to the test results of this study. Different strain rates that correspond to the critical damage (D_c) are shown in Figure 13. The strains considerably vary when the critical damage approaches under different strain rates, but the critical damage value (D_c) differs a little. This result suggests that the plastic strain, elastic strain, and their contributions to the total deformation are independent of the deformation degree and strain rate.

4.2.3. Energy Dissipation Method. According to thermodynamics and fracture mechanics, the work performed by external loads is not entirely stored as elastic strain energy under the isothermal and adiabatic condition, and a part of it is consumed in damage nucleation and evaluation. For

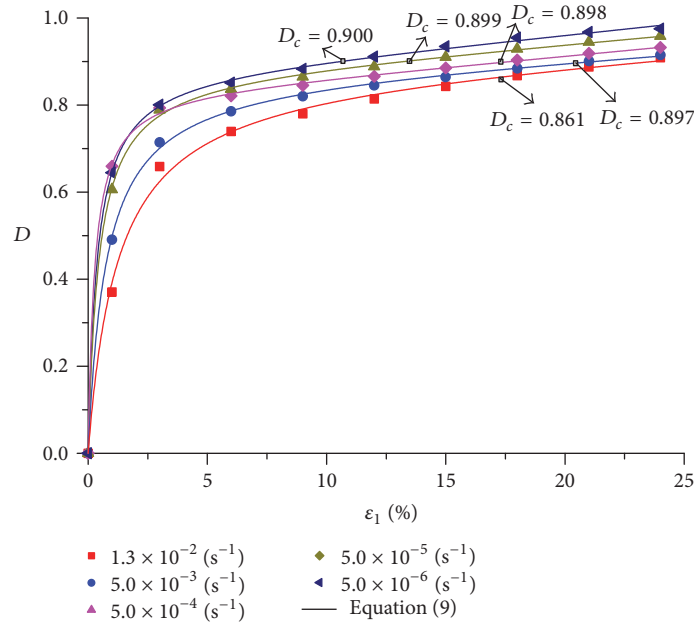


FIGURE 11: Variation of the damage variable with axial strain under different strain rates (stiffness).

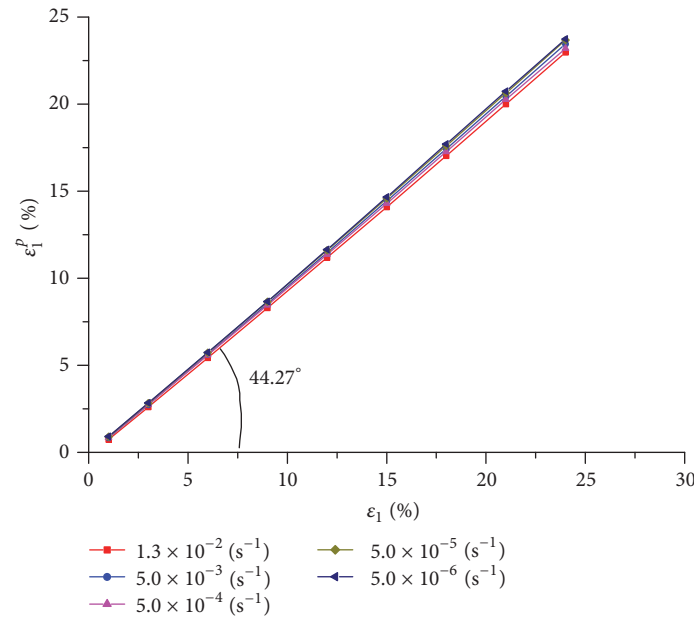


FIGURE 12: Variation of the plastic strain with axial strain under different strain rates.

convenience, it is a hypothesis that the dissipated energy can contribute to the development of material damage according to the view of J integral in fracture mechanics. Thus, the dissipated energy can also be treated as a damage factor for the damage evolution. Regarding the dissipated energy, the hysteresis loop area W_h of loading and unloading curves is commonly considered the dissipated energy of the material [6].

According to the principle of energy conservation and damage evolution, the initial damage of the specimen should

be selected as the reference point of damage evolution. However, the hysteresis loop area is only the dissipated energy of one loading-unloading cycle (the dissipated energy within the rebound strain) [29].

Based on the test results in this study, the variation of the hysteresis loop area of frozen loess with axial strain under different strain rates is shown in Figure 14. The area of the hysteresis loop decreases after the peak strain because the shear failure of the frozen loess mesostructure makes the strength reduction. Then, the hysteresis loop area cannot

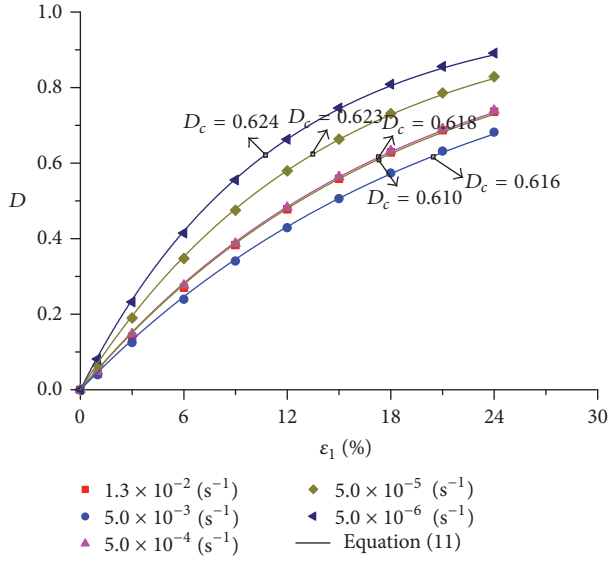


FIGURE 13: Variation of the damage variable with axial strain under different strain rates (plastic strain).

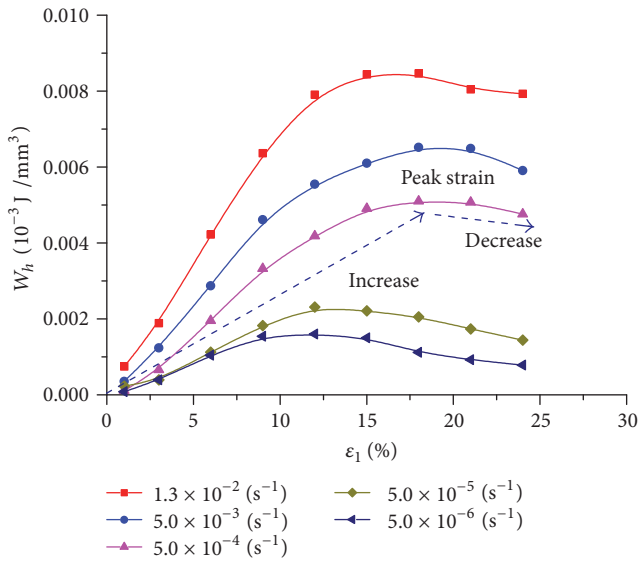


FIGURE 14: Variation of the hysteresis loop area with axial strain under different strain rates.

accurately reflect the mesofailure process of frozen loess. The test results again indicate that the hysteresis loop area could not be directly considered the damage factor.

Based on the view of fracture mechanics and energy conservation, the dissipated energy is recalculated as follows:

$$W = W_s + W_b + W_r, \quad (12)$$

where W_s is the storage elastic energy of the testing system during loading; W_b is the dissipated energy of the testing machine damping; and W_r is the absorbed energy by the specimen. W_s , W_b can be ignored because the stiffness of the testing machine is far greater than the frozen loess specimen.

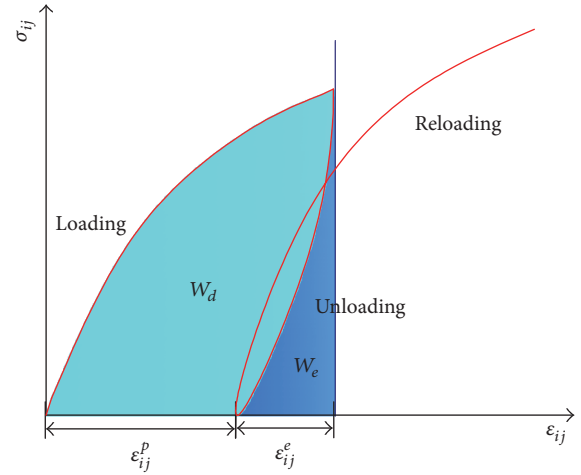


FIGURE 15: The calculation method of dissipated energy (ϵ_{ij}^p is the plastic strain).

Then, the entire work (W) can be considered absorbed by the specimen (W_r). In the isothermal and adiabatic conditions, one part of the work performed by external loads is stored in the form of elastic energy (W_e), which is released after unloading. Another part of the work is consumed by the development of plastic deformation and cracks based on Huang and Li [20]. Thus, this part can also be called the dissipated energy (W_d).

$$W \approx W_r = W_e + W_d = \int_0^\epsilon \sigma_{ij} d\epsilon_{ij} \quad (13)$$

$$W_e = \int_s \sigma_{ij} d\epsilon_{ij}^e,$$

where s is the unloading path and ϵ_{ij}^e is the elastic strain. Then, the dissipated energy can be calculated from the $L-U-C$ test results, and the calculation method is shown in Figure 15.

The variation of dissipated energy with axial strain is shown in Figure 16. The dissipated energy increases with the increase in axial strain. With the increase in dissipated energy, the cracks and holes in the specimen increase, and the specimen eventually achieves the extreme damage status. Considering the irreversibility of the damage, the damage variable can be expressed as follows:

$$D = \frac{\sum_{i=1}^n W_d^i}{W_d^u}, \quad (14)$$

where W_d^u is the dissipated energy of the specimen corresponding to the critical damage; W_d^i is the dissipated energy under different damage stages. The relationship between the damage variable and the axial strain is shown in Figure 17. Based on the test results of this study and Darabi et al. [15], the damage evolution law can be written as follows:

$$D = \alpha \left(\frac{\epsilon_1}{\epsilon_1^u} \right) \exp \left(\beta \frac{\epsilon_1}{\epsilon_1^u} \right), \quad (15)$$

TABLE 4: Material parameters α and β under different strain rates (dissipated energy).

$\dot{\epsilon}_1$	$1.3 \times 10^{-2}/s$	$5.0 \times 10^{-3}/s$	$5.0 \times 10^{-4}/s$	$5.0 \times 10^{-5}/s$	$5.0 \times 10^{-6}/s$
α	0.415	0.482	0.369	0.468	0.474
β	0.881	0.748	1.001	0.773	0.760

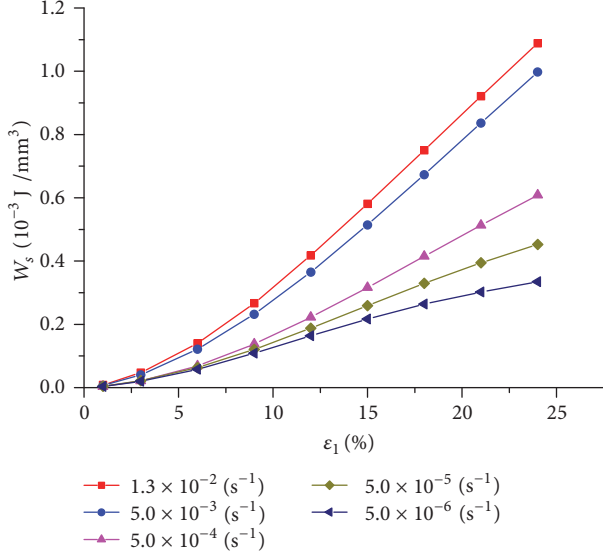


FIGURE 16: Variation of dissipated energy with axial strain under different strain rates.

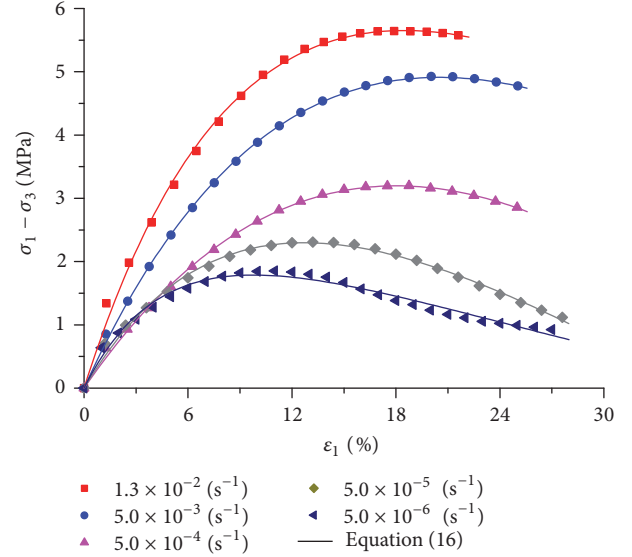


FIGURE 18: The model matches effect.

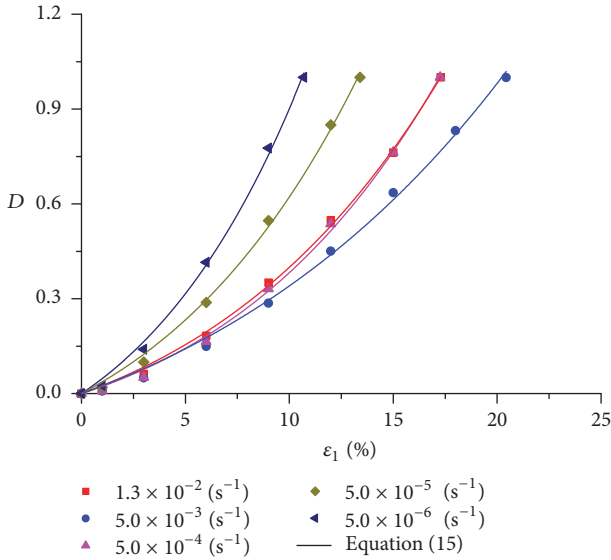


FIGURE 17: Variation of the damage variable with axial strain under different strain rates (dissipated energy).

where α and β are material parameters corresponding to the strain rate. These parameters under different strain rates are listed in Table 4.

4.2.4. *Damage Evolution Laws Deduced from the Constitutive Model.* The constitutive model of some materials has been

known, but the damage evolution law cannot be clearly observed from the model. Then, the damage evolution law can be deduced from the constitutive model. Bažant and Mazars [25] and Lemaitre [30] calculated the damage of a material by fitting stress-strain curves according to the phenomenological theory.

Considering the deformation features of frozen loess, a generalized hyperbolic model is used in this study [31]. With the model, the C test results are fitted, as shown in Figure 18.

$$\sigma_1 - \sigma_3 = \frac{l + m\epsilon_1}{(l + n\epsilon_1)^2} \epsilon_1 = (1 - D) E_0^* \epsilon_1 \quad (16)$$

$$\frac{\sigma}{(1 - D)} = \sigma_{\text{eff}}, \quad (17)$$

where E_0^* is the initial modulus that corresponds to the fitting curves; l , m , and n are material parameters that are related to the strain rate. These parameters under different strain rates are listed in Table 5. The physical significance of these parameters can be found in Prévost [31]. The methods can characterize stiffness degradation of material by modulus (16) and the strength change of material by the effective stress (17) in the deformation process. The two variables can be deduced from the same method [23]. In the paper, we used the modulus as an example.

Then, the equation of damage evolution can be obtained as follows:

$$D = 1 - \frac{l + m\epsilon_1}{E_0^* (l + n\epsilon_1)^2}. \quad (18)$$

TABLE 5: Material parameters l , m , and n under different strain rates (constitutive model).

$\dot{\epsilon}_1$	$1.3 \times 10^{-2}/s$	$5.0 \times 10^{-3}/s$	$5.0 \times 10^{-4}/s$	$5.0 \times 10^{-5}/s$	$5.0 \times 10^{-6}/s$
l	0.01159	0.01660	0.02520	0.02200	0.01800
m	-0.01853	-0.03000	-0.06200	-0.06200	-0.04540
n	0.02570	0.02090	0.01660	0.04720	0.09450

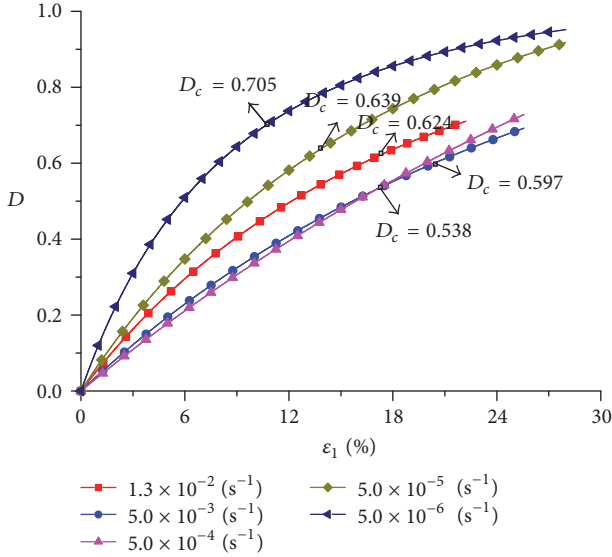


FIGURE 19: Variation of the damage variable with axial strain under different strain rates (constitutive model).

The variation of the damage variable with axial strain is shown in Figure 19. The development of damage is closely related to the loading time, which is consistent with the results of the C tests. The critical damage (D_c) is shown in Figure 19.

5. Discussion

At present, few studies compared the advantages and disadvantages among different damage factors or discussed the selection criteria of the damage variable to the same material. In this paper, four damage factors were studied and compared based on macro tests results of frozen loess. Based on the above studies, the four methods can describe the damage and damage evolution of frozen loess under ideal conditions. However, considering the special properties and engineering service purposes on frozen loess, the advantages and disadvantages of these damage factors and damage variables will be assessed as follows.

For frozen loess, it is difficult to accurately measure the dissipated energy by experiments, and it is not for presenting the damage process considering the special physical property of the granular material [32]. In the paper, the dissipated energy of the frozen loess was calculated based on many hypotheses. Thus, the dissipated energy is hardly investigated and not recommended in this area. The fourth method is that the damage evolution law is obtained from the constitutive model based on the theory of effective stress, but the premise

is that the constitutive model of the material is known. Because of the complexity of the geotechnical property, such as large regional characteristics and the complex structure, it is difficult to obtain a simple and accurate model. Therefore, this method is also difficult to apply. The theory of stiffness degradation can be used for most materials and the stiffness of material is also easy to measure. Thus, many researchers choose the stiffness as the damage factor to study the mechanical damage of material. The main limitation of the method is that damage is uniformly distributed in the volume on which strain is measured. Thus, it is also difficult regarding frozen loess. For frozen loess engineering, the key engineering problem is the deformation issue, for example, subgrade settlement and foundation deformation, which is the safety evaluation index to these engineering. Therefore, plastic deformation (permanent deformation) is the most suitable for the damage research of frozen loess based on the material properties and the nature of the material service.

In addition, the problem of establishing a quantitative relationship between the damage factor and the damage variable for different materials and different purposes should be considered. Different relationships lead to different evolution processes, such as the comparison results of the exponential function (10) and linear function ((6) and (14)). The key point to understand is how to exactly define the damage criterions.

Selecting an appropriate damage factor has been a hot topic for a long time in CDM. Based on this discussion, it can be seen that a new technology (microscopic scanning) and method must be developed to more accurately describe the damage evolution of the material under external loads. The method is a comprehensive method that contains macro- and micromethods (the combination of material science and continuous media mechanics or mechanical damage and physical damage). Both methods are essential; otherwise, the damage process of the material can only be described from one side. In other words, the method must be able to verify and inverse the macromechanical properties of the material according to the change law of mesoscopic fabric status. Selecting a cross-scale damage variable is also the key bridge to explore the essence of deformation and failure of materials. This subject is also a main issue of the study of material properties in current solid mechanics [33].

6. Conclusions

This paper presented a series of tests, including monotonic and load-unloading-loading tests, to the frozen loess under five strain rates in order to investigate the rate-dependent deformation behavior and the damage evolution law. Four damage factors were studied and compared based on tests

results. Some conclusions drawn from experimental and theoretical results are summarized below.

(1) The strength and the deformation behavior of frozen loess strongly depend on the strain rate. In addition, the loading and unloading cycles test does not affect the deformation behavior of frozen loess.

(2) E_h and E_s cannot describe the stiffness degradation of the frozen loess in the deformation process. So E_d is selected based on the test results and previous studies.

(3) The hysteresis loop area cannot accurately reflect the dissipated energy of frozen loess. The value of dissipated energy is recalculated according to the view of fracture mechanics and energy conservation in order to describe the development of the material damage.

(4) According to the discussion, the plastic deformation is the most suitable for the damage research of frozen loess based on the material properties and the nature of the material service.

Conflicts of Interest

The authors declare that there are no conflicts of interest regarding the publication of this paper.

Acknowledgments

This work was supported by the National Natural Science Foundation of China (41630636, 41401077, and 11502266) and the Science and Technology Major Project of Gansu Province (143GKDA007).

References

- [1] J. Q. Xu, *Theory on the Strength of Materials*, Shanghai Jiaotong University Press, 2009.
- [2] R. A. Schapery, "Correspondence principles and a generalized J integral for large deformation and fracture analysis of viscoelastic media," *International Journal of Fracture*, vol. 25, no. 3, pp. 195–223, 1984.
- [3] S. Dhar, P. M. Dixit, and R. Sethuraman, "A continuum damage mechanics model for ductile fracture," *International Journal of Pressure Vessels and Piping*, vol. 77, no. 6, pp. 335–344, 2000.
- [4] R. W. Sullivan, "Development of a viscoelastic continuum damage model for cyclic loading," *Mechanics of Time-Dependent Materials*, vol. 12, no. 4, pp. 329–342, 2008.
- [5] S. P. Zhao, W. Ma, J. F. Zheng, and G. D. Jiao, "Damage dissipation potential of frozen remolded Lanzhou loess based on CT uniaxial compression test results," *Chinese Journal of Geotechnical Engineering*, vol. 34, pp. 2019–2025, 2012.
- [6] X. T. Xu, Y. H. Dong, and C. X. Fan, "Laboratory investigation on energy dissipation and damage characteristics of frozen loess during deformation process," *Cold Regions Science and Technology*, vol. 109, pp. 1–8, 2015.
- [7] J. Shao, A. Chiarelli, and N. Hoteit, "Modeling of coupled elastoplastic damage in rock materials," *International Journal of Rock Mechanics and Mining Sciences*, vol. 35, no. 4–5, p. 444, 1998.
- [8] J. Lemaitre, "Continuous damage mechanics model for ductile fracture," *Journal of Engineering Materials and Technology, Transactions of the ASME*, vol. 107, no. 1, pp. 83–89, 1985.
- [9] G. Z. Voyiadjis, *Handbook of Damage Mechanics*, Springer, 2015.
- [10] M. Alves, J. Yu, and N. Jones, "On the elastic modulus degradation in continuum damage mechanics," *Computers and Structures*, vol. 76, no. 6, pp. 703–712, 2000.
- [11] G. Swoboda and Q. Yang, "An energy-based damage model of geomaterials—I. Formulation and numerical results," *International Journal of Solids and Structures*, vol. 36, no. 12, pp. 1719–1734, 1999.
- [12] R. Lapovok, "Damage evolution under severe plastic deformation," *International Journal of Fracture*, vol. 115, no. 2, pp. 159–172, 2002.
- [13] Z. M. Shi, H. L. Ma, and J. B. Li, "A novel damage variable to characterize evolution of microstructure with plastic deformation for ductile metal materials under tensile loading," *Engineering Fracture Mechanics*, vol. 78, no. 3, pp. 503–513, 2011.
- [14] Y. Y. Cao, S. P. Ma, X. Wang, and Z. Y. Hong, "A new definition of damage variable for rock material based on the spatial characteristics of deformation fields," *Advanced Materials Research*, vol. 146–147, pp. 865–868, 2011.
- [15] M. K. Darabi, R. K. Abu Al-Rub, E. A. Masad, C.-W. Huang, and D. N. Little, "A thermo-viscoelastic-viscoplastic-viscodamage constitutive model for asphaltic materials," *International Journal of Solids and Structures*, vol. 48, no. 1, pp. 191–207, 2011.
- [16] H. Du, W. Ma, S. Zhang, Z. Zhou, and E. Liu, "Strength properties of ice-rich frozen silty sands under uniaxial compression for a wide range of strain rates and moisture contents," *Cold Regions Science and Technology*, vol. 123, pp. 107–113, 2016.
- [17] Z. Zhou, W. Ma, S. Zhang, H. Du, Y. Mu, and G. Li, "Multiaxial creep of frozen loess," *Mechanics of Materials*, vol. 95, pp. 172–191, 2016.
- [18] L. M. Kachanov, *Introduction to Continuum Damage Mechanics*, M. Nijhoff, 1986.
- [19] L. M. Kachanov, "Time of the rupture process under creep conditions," *Akad. Nauk SSR Otd. Tech.*, vol. 8, p. 6, 1958.
- [20] D. Huang and Y. Li, "Conversion of strain energy in Triaxial Unloading Tests on Marble," *International Journal of Rock Mechanics and Mining Sciences*, vol. 66, pp. 160–168, 2014.
- [21] A. S. Chiarelli, J. F. Shao, and N. Hoteit, "Modeling of elastoplastic damage behavior of a claystone," *International Journal of Plasticity*, vol. 19, no. 1, pp. 23–45, 2003.
- [22] G. E. Mann, T. Sumitomo, C. H. Cáceres, and J. R. Griffiths, "Reversible plastic strain during cyclic loading-unloading of Mg and Mg-Zn alloys," *Materials Science and Engineering A*, vol. 456, no. 1–2, pp. 138–146, 2007.
- [23] H. P. Xie, *Rock and Concrete Damage Mechanics*, China University of Mining and Technology Press, 1990.
- [24] S. W. Yu, *Damage Mechanics*, Tsinghua University Press, 1997.
- [25] Z. P. Bažant and J. Mazars, "France-U.S. workshop on strain localization and size effect due to cracking and damage," *Journal of Engineering Mechanics*, vol. 116, no. 6, pp. 1412–1424, 1990.
- [26] I. Carol, E. Rizzi, and K. Willam, "A unified theory of elastic degradation and damage based on a loading surface," *International Journal of Solids and Structures*, vol. 31, no. 20, pp. 2835–2865, 1994.
- [27] J. Lemaitre, *A Course on Damage Mechanics*, Springer, 1998.
- [28] M. Liao, Y. Lai, E. Liu, and X. Wan, "A fractional order creep constitutive model of warm frozen silt," *Acta Geotechnica*, pp. 1–13, 2016.
- [29] Y. Yugui, G. Feng, C. Hongmei, and H. Peng, "Energy dissipation and failure criterion of artificial frozen soil," *Cold Regions Science and Technology*, vol. 129, pp. 137–144, 2016.

- [30] J. Lemaitre, "Formulation and identification of damage kinetic constitutive equations," in *Continuum Damage Mechanics Theory and Application*, vol. 295 of *International Centre for Mechanical Sciences*, pp. 37–89, Springer, Vienna, Austria, 1987.
- [31] J. Prévost, "Mathematical modelling of monotonic and cyclic undrained clay behaviour," *International Journal for Numerical and Analytical Methods in Geomechanics*, vol. 1, no. 2, pp. 195–216, 1977.
- [32] J. Lemaitre and J. Dufailly, "Damage measurements," *Engineering Fracture Mechanics*, vol. 28, no. 5-6, pp. 643–661, 1987.
- [33] F. Hild, A. Bouterf, and S. Roux, "Damage measurements via DIC," *International Journal of Fracture*, vol. 191, no. 1-2, pp. 77–105, 2015.



Hindawi

Submit your manuscripts at
<https://www.hindawi.com>

